B. TECH. PROJECT REPORT

On

Evaluation of RRAM Models for Data Processing and Security Applications

BY

Rajan Agrawal

DISCIPLINE OF ELECTRICAL ENGINEERING

INDIAN INSTITUTE OF TECHNOLOGY INDORE

December 2019

Evaluation of RRAM Models for Data Processing and Security Applications

A PROJECT REPORT

Submitted in partial fulfillment of the requirements for the award of the degrees of

BACHELOR OF TECHNOLOGY
in

ELECTRICAl ENGINEERING

Submitted by:
Rajan Agrawal
Guided by:
Dr. Shaibal Mukherjee
Associate Professor
Department of Electrical Engineering

INDIAN INSTITUTE OF TECHNOLOGY INDORE
December 2019

CANDIDATE'S DECLARATION

I hereby declare that the project entitled **"Evaluation of RRAM Models for Data Processing and Security Applications"** submitted in partial fulfillment for the award of the degree of Bachelor of Technology in 'Electrical Engineering' completed under the supervision of **Dr. Shaibal Mukherjee, Associate Professor, Electrical Engineering,** IIT Indore is an authentic work.

Further, I declare that I have not submitted this work for the award of any other degree elsewhere.

Signature and name of the student(s) with date

CERTIFICATE by BTP Guide(s)

It is certified that the above statement made by the students is correct to the best of my knowledge.

Signature of BTP Guide(s) with dates and their designation

Preface

This report on "Evaluation of RRAM Models for Data Processing and Security Applications" is prepared under the guidance of Dr. Shaibal Mukherjee.

Through this report we have tried to give a generic analytical model of a memristive device and try to take into account the non-idealities shown by the actual devices. We have tried to the best of our abilities and knowledge to explain the content in a lucid manner. We have also added various illustrations and data tables to make it more illustrative. The MATLAB platform has been used for coding the models and ORIGIN has been used for subsequent curve fitting.

Rajan Agrawal
B.Tech. IV Year
Discipline of Electrical Engineering
IIT Indore

Acknowledgements

I wish to thank Dr. Shaibal Mukherjee for his kind support and valuable guidance.

It is his help and support, due to which I was able to complete the design and technical report..

Also I thank all the members of HNRG lab for their support and cooperation in facilitation of experimental data for analytical modeling.

Without their support this report would not have been possible.

Rajan Agrawal
B.Tech. IV Year
Discipline of Electrical Engineering
IIT Indore

Abstract

In recent years, memristor has been recognized as the fourth fundamental circuit element apart from resistor, inductor and capacitor. One of the major applications of memristor is Resistive Random Access Memory (RRAM). This has proved to be a promising candidate for the replacement of conventional charge based memory technology in future data storage applications. Also memristor can be utilized in development of artificial neural network thus imitating the efficiency of biological systems.

Most of the experimental data reported in the literature for various material systems such as WO3 , Y2O3, ZnO etc shows asymmetric behavior in the pinched hysteresis loop in the current-voltage (I-V) characteristics. However, till date, to our knowledge, a detailed analytical model is unavailable which could be matched with such experimental hysteresis loop due to various non idealities shown by practical devices which could be used to analyze the system performance.

Our work involved analytical modeling based on two different already proposed models: Yakopcic model and non -linear ion drift model. We have tried to remove limitations of both the models by introducing certain fitting parameters and checking the correlation with the experimental data already reported. A new window function has been introduced in the non linear model in order to improve characteristic behavior at the device boundaries. The second model gave significant improvement over the first model and thus achieving our objective.

In this thesis work, the first chapter focuses on study of Yakopcic model and the effects of all the parameters on the device characteristics. Next, we focus on the significance of the modifications made in the model to improve the device behavior and arrive at a better correlation with experimental data. The effects of various elementary functions like window functions on state variable have been analyzed to measure their impact on the device characteristics and the parameters determining their suitability for a current –voltage relation is critically analyzed.

The next part of the work focuses on another memristor model called non -linear ion drift model and proposing a new window function. The modifications have been introduced to decrease the error margin and the new model is evaluated with the experimental data. Next, we present the results, discussions and their significance where suitable illustrations have been provided for comprehension.

The subsequent part focuses on the applicability part of the work and discusses conclusion and future scope of the work.

Table of contents

<u>Chapter 1</u>

Yakopcic model

Memristor is a two-terminal electrical passive component that exhibits pinched hysteresis characteristic between voltage and current [5] and also indicates various interesting non-linear characteristics. The dynamics of a memristive device were found much closer to a synapse thus it can be considered an ideal neuromorphic system. As in a biological system, during synaptic activity, an action potential triggers the presynaptic neuron to release neurotransmitters, memristive devices exhibit various such properties analogous to forgetting and learning experience behavior of a human memory. Thus it is needed to design a model for simulating these synaptic applications of a memristor.

Thus, we start by simulating an already proposed mathematical model by Yakopcic [2] and comparing these results with the characterized data of Y_2O_3 based memristive devices [1]. The Yakopcic model has shown discrepancy when comparing these results with the characterized data.

After suitable modifications we are able to implement the neuromorphic behavior on the model by simulating the Potentiating and Depressing curves.

Details of the Yakopcic Model

Equation (1) describes the current-voltage (*I-V)* relationship for the Yakopcic model.

$$I(t) = \begin{Bmatrix} a_1 x(t)\, sinh\big(bV(t)\big), & V(t) \geq 0 \\ a_2 x(t)\, sinh\big(bV(t)\big), & V(t) < 0 \end{Bmatrix} \qquad (1)$$

This model utilizes certain fitting parameters like a_1, a_2 and b to fit the response of different memristor devices. The fitting parameter b controls the slope of conductivity with respect to magnitude of applied voltage. Here $x(t)$ represents the state variable whose value is bound from 0 to 1. It provides a significant change in device conductance as its value varies.

Two different functions $g(V(t))$ and $f\big(x(t)\big)$ are defined to control the variation in $x(t)$.

$$g\big(V(t)\big) = \begin{Bmatrix} A_{\mathrm{p}}\big(e^{V(t)} - e^{V_{\mathrm{p}}}\big), & V(t) > V_{\mathrm{P}} \\ -A_{\mathrm{n}}\big(e^{-V(t)} - e^{V_{\mathrm{n}}}\big), & V(t) < -V_{\mathrm{n}} \\ 0, & -V_{\mathrm{n}} \leq V(t) \leq V_{\mathrm{p}} \end{Bmatrix} \qquad (2)$$

$$f(x) = \begin{cases} e^{-\alpha_{\mathrm{p}}(x-x_{\mathrm{p}})} W_{\mathrm{p}}(x,\ x_{\mathrm{p}}), & x \geq x_{\mathrm{p}} \\ 1\ , & x < x_{\mathrm{p}} \end{cases} \tag{3}$$

$$f(x) = \begin{cases} e^{\alpha_{\mathrm{n}}(x+x_{\mathrm{n}}-1)} W_{\mathrm{n}}(x,\ x_{\mathrm{n}}), & x \leq 1 - x_{\mathrm{n}} \\ 1\ , & x > 1 - x_{\mathrm{n}} \end{cases} \tag{4}$$

When $V(t) > 0$, the variation in state variable is defined by equation (3); otherwise, the variation is defined by equation (4).

Here V_{p} and V_{n} represent the positive and negative thresholds for the applied input voltage. The functions $g(V(t))$ and $f(x(t))$ are defined as the programming threshold function and state variable function, respectively, for the memristor model. Here, $\mathrm{W_p}$ and $\mathrm{W_n}$ are the window functions and described by equations 5 and 6, respectively

$$W_{\mathrm{p}}(x,\ x_{\mathrm{p}}) = \frac{x_{\mathrm{p}}-x}{1-x_{\mathrm{p}}} + 1 \tag{5}$$

$$W_{\mathrm{n}}(x,\ x_{\mathrm{n}}) = \frac{x}{1-x_{\mathrm{n}}} \tag{6}$$

These window functions control the effect of the state variable at the boundaries (i.e. at $x = 0$ & $x = 1$). They ensure to keep the value of the state variable bounded within the limits.

Equation (7) is used to depict the rate of variation of the state variable with respect to time in the memristive devices.

$$\frac{dx}{dt} = g\big(V(t)\big) * f\big(x(t)\big) \tag{7}$$

<u>**Proposed Model**</u>

I-*V* relationship for the proposed model after modifications is given by (8).

$$I(t) = \begin{cases} a_1 x(t)\, sinh\big(b_1 V(t)\big), & V(t) \geq 0 \\ a_2 x(t)\, sinh\big(b_2 V(t)\big), & V(t) < 0 \end{cases} \tag{8}$$

Where, a_1 and a_2 are the parameters for experimental fitting, $\mathrm{b_1}$ and $\mathrm{b_2}$ are the parameters for controlling the conductivity slope for the positive and negative applied voltage, respectively. In order to facilitate better control on device hysteresis loop, separate conductivity control parameters have been provided in the simplified model. Thus we can say the modified equation is applicable for both unipolar and bipolar devices whereas the earlier equations were taking into consideration only bipolar devices.

Here equation (9) represents the rate of change of state variable

$$\frac{dx}{dt} = \begin{Bmatrix} G(V(t))e^{-\alpha_{\mathrm{p}}U(x-x_{\mathrm{p}})(x-x_{\mathrm{p}})}\left(1+(W_{\mathrm{p}}-1)U(x-x_{\mathrm{p}})\right), & V(t)>0 \\ G(V(t))e^{\alpha_{\mathrm{n}}U(x_{\mathrm{p}}-x)(x-x_{\mathrm{p}})}\left(1+(W_{\mathrm{n}}-1)U(x_{\mathrm{p}}-x)\right), & V(t)<0 \end{Bmatrix} \qquad (9)$$

This depends on various parameters like $\alpha_{\mathrm{p}},\ \alpha_{\mathrm{n}},\ W_{\mathrm{p}},\ W_{\mathrm{n}},\ x,$ and $U(t)$

$$G(V(t)) = \begin{Bmatrix} A_{\mathrm{p}}\left(e^{V(t)}-1\right), & V(t)>0 \\ -A_{\mathrm{n}}\left(e^{-V(t)}-1\right), & V(t)<0 \end{Bmatrix} \qquad (10)$$

In the proposed model we have imposed one more condition on window function, i.e., $x_{\mathrm{p}} + x_{\mathrm{n}} = 1$ and are described by equations (11 and 12).

$$W_{\mathrm{p}} = \frac{x_{\mathrm{p}}-x}{x_{\mathrm{n}}} + 1 \qquad (11)$$

$$W_{\mathrm{n}} = \frac{x}{x_{\mathrm{p}}} \qquad (12)$$

By utilizing this relation, we are able to eliminate the variable x_{n} and try to derive all the curve fittings utilizing these equations with reduced variables.

Effects of various parameters

(I)

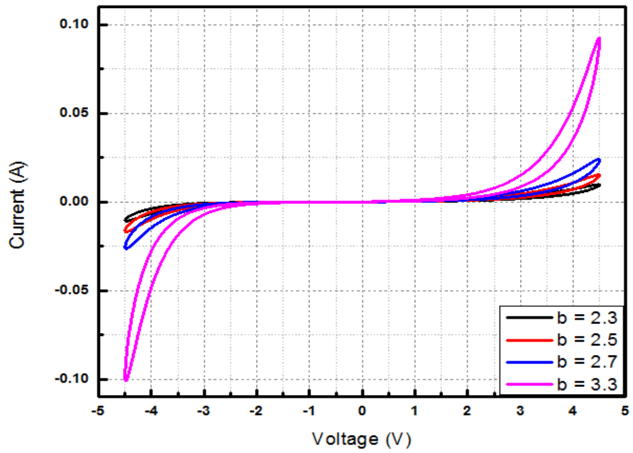

Fig.1 Effect of Fitting Parameter (b) on Pinched Hysteresis I-V Plot

Since b is the parameter controlling the current magnitude , its value determines the area of the loop and its boundary behavior.

(II)

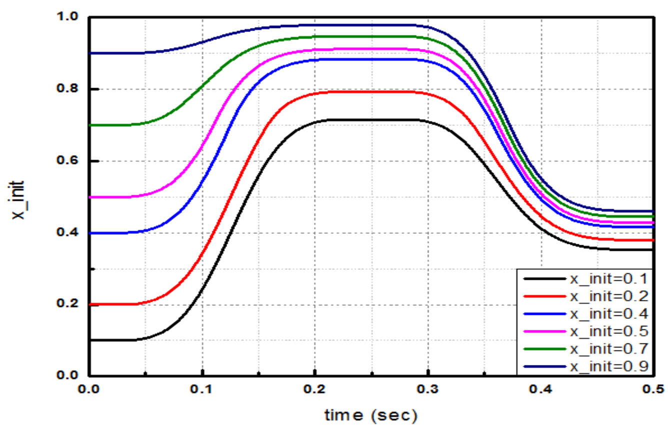

Fig.2 Variation in State Variable x_init with Time

Here as we change the value of initial state variable from low to high the state variation curve shifts from low to high. Thus we observe that devices with higher initial state value depict higher conductance at all values of input voltages. Here the state variable represents the length of conductive region relative to total device length thus it represents a variable in one dimension.

(III)

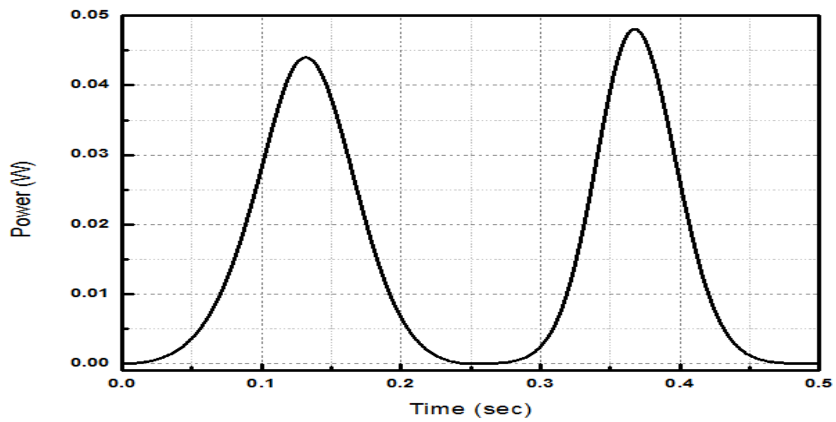

Fig.3 Variation in Power with Respect to Time

Here we plot the instantaneous power at various time instants. For one cycle of triangular/ sinusoidal pulse, we obtain two cycles of power variation from minimum to maximum, each in one polarity of quadrant. The two lobes may be symmetric/ asymmetric depending on the behavior of hysteresis loop.

(IV)

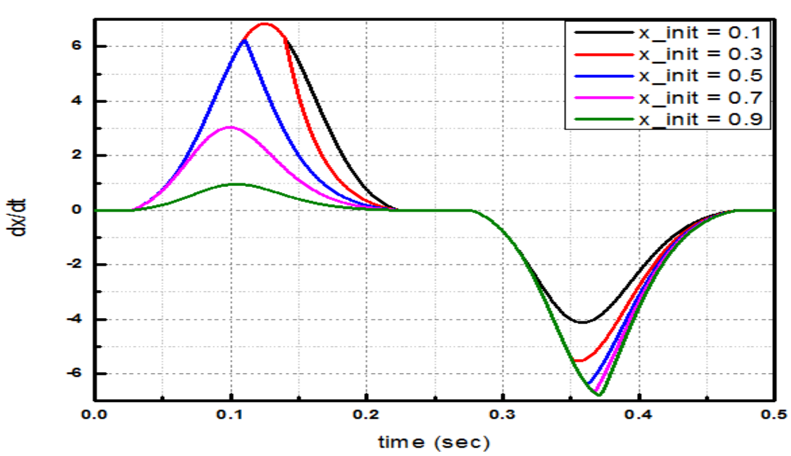

Fig.4 Variation in $\frac{dx}{dt}$ with Time at Different Values of x_init

Here we observe that higher values of initial state variables lead to higher values of current response of the device at all subsequent time intervals.

(V)

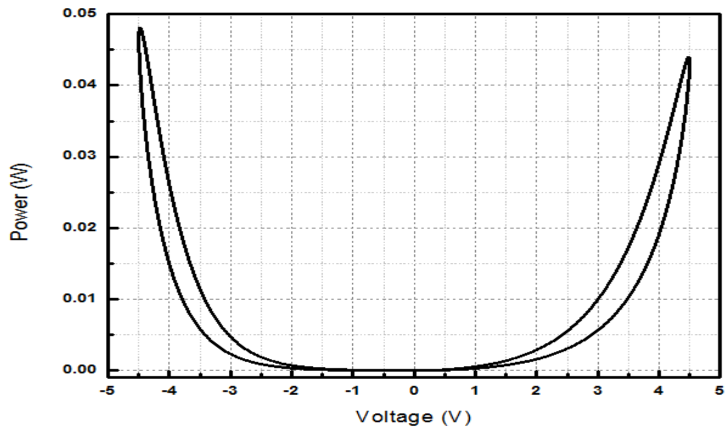

Fig.5 Variation in Instantaneous Power with Respect to Voltage

Here we plot the instantaneous power in the form of product of input voltage and current response. As illustrated, maximum power dissipation takes place at the device boundary when the value of the state variable is at its maximum.

(VI)

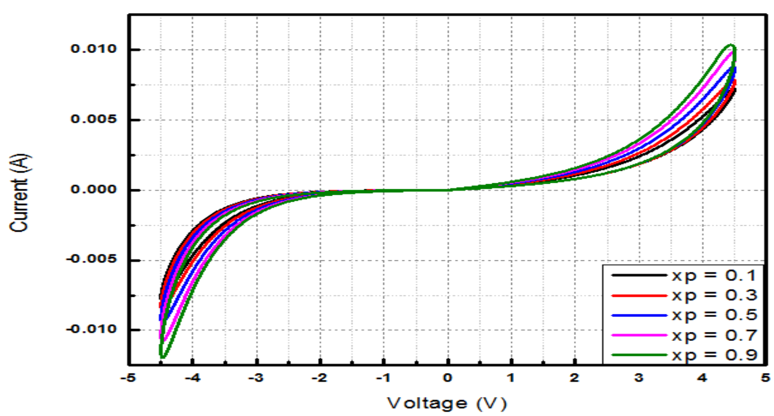

Fig.6 Effect of State Constant (x_p) on Pinched Hysteresis I-V Plot

Here (x_p) represents the state constant which actually sets the limit of the state variable for various values of rate of change of state variable with respect to time. As we change the value of (x_p) the state threshold changes thus changing the shape of the waveform.

Results and Discussions

(I)

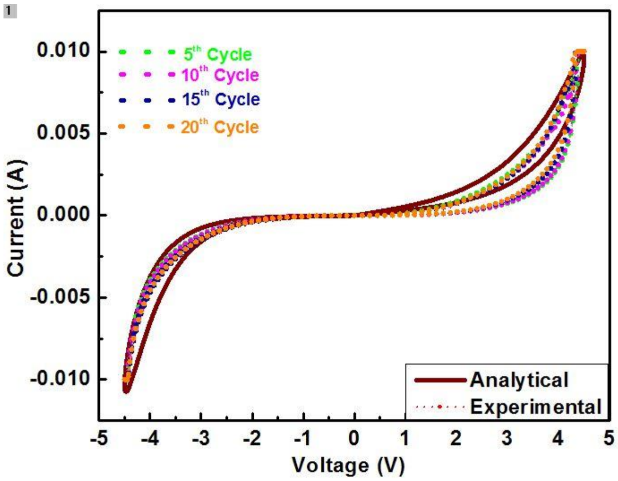

Fig.7 I-V Characteristics

Here different cycles of hysteresis loops are matched with corresponding cycle of simulated model and curves are fitted by changing suitable parameters.

(II)

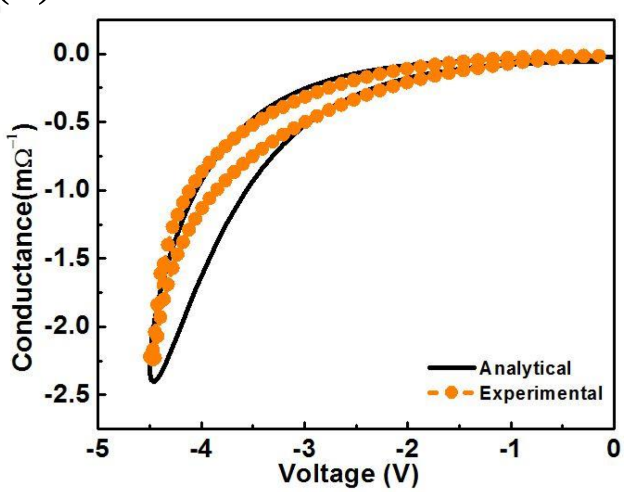

Fig.8. Conductance vs Voltage

Here conductance (i.e. the ratio of current and voltage) is plotted against voltage for negative cycle of input applied and the deviation from the experimental data is observed.

(III)

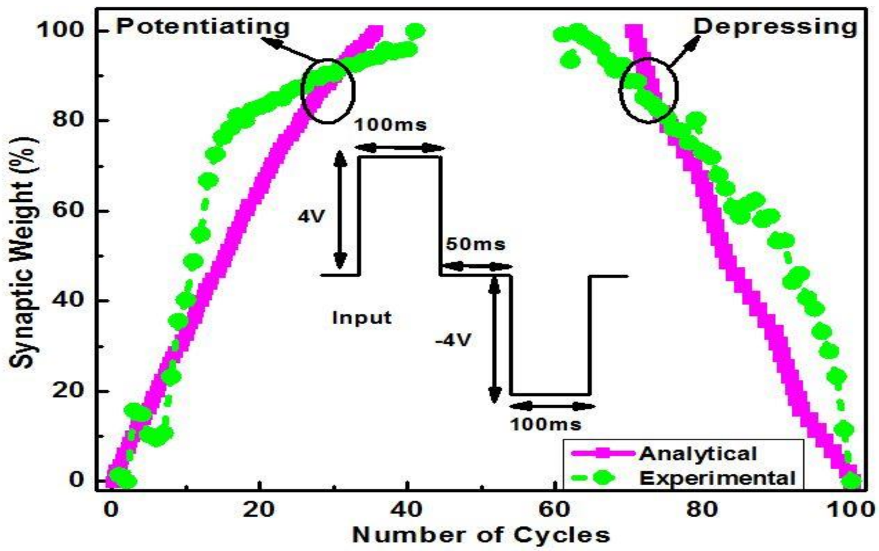

Fig.9 Synaptic Weight vs number of cycles

Here Potentiating and Depressing curves are drawn for the memristor model by application of the given input voltage. The curves obtained are plotted simultaneously with experimental curves.

(IV)

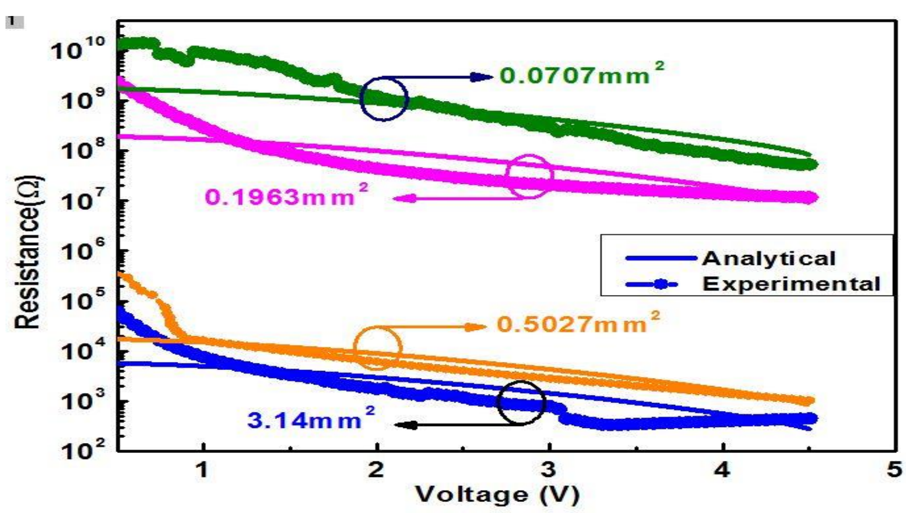

Fig.10 Resistance vs voltage for different areas

This curve demonstrates that resistance of the device is inversely proportional to the area of cross section of the device. The below drawn curve mentions the same phenomenon in terms of current vs applied input waveform for different areas.

(V)

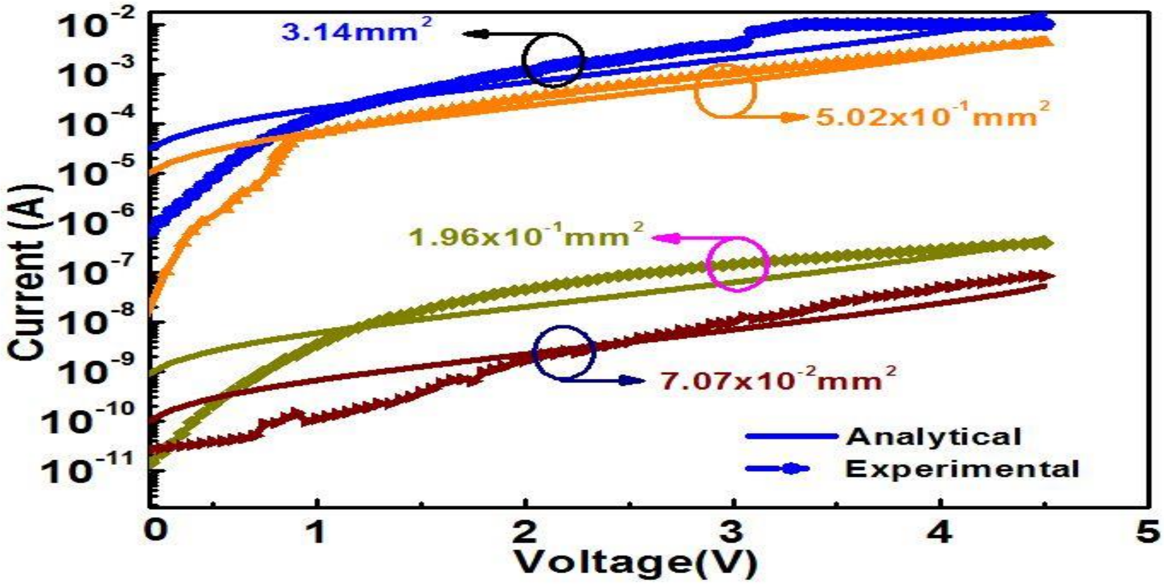

Fig.11 Current vs Voltage for different areas

(VI)

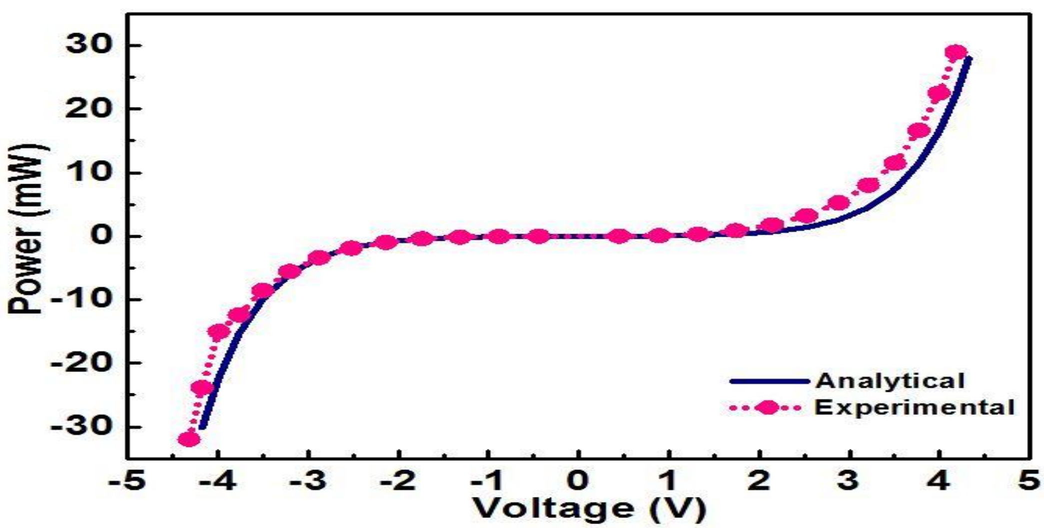

Fig.12 Actual Power vs Voltage

The actual power consumption in the switching cycle for different voltage levels is demonstrated by the above figure.

TABLE.1

Various parameter values and their physical interpretation

Parameters	**Numerical Values**	**Physical Interpretation**
a_1	$7e^{-4}$	Experimental fitting parameter
a_2	$3.9e^{-5}$	Experimental fitting parameter
b_1	3.8	Parameter controlling conductivity for positive voltage polarity
b_2	1.5	Parameter controlling conductivity for negative voltage polarity
α_p, α_n	1.2	Parameters controlling the rate of change of state variable
x_p	0.7	Constant for determining the bounded nature of state variable
x_n	0.3	Constant for determining the bounded nature of state variable
A_p, A_n	0.0021	Magnitude of exponentials

Chapter 2
Non Linear Model

For a large region of memristor voltages, the devices show non linear behavior at the boundaries. In order to account for such non linear characteristics, several analytical models have been proposed . But such models mostly simulate results showing symmetric behavior in positive and negative half cycles. Here considering the already proposed non linear model as reference, we try to propose a new model with a different logarithmic window function and curve fit the results using the experimental data of Y_2O_3.

Equation (1) represents the current voltage relationship for the already proposed non linear model [4]

$$I(t) = W^n\beta\, sinh(\alpha V_{\mathrm{i}}(t)) + X\{e^{\gamma V_{\mathrm{i}}(t)} - 1\} \qquad (1)$$

Here the first part of the equation indicates the tunneling phenomenon and is responsible for nonlinear behavior and the second part shows the ideal diode behavior.

Here W represents the normalized state variable bounded from 0 to 1

Equation (2) shows the current voltage relation for the proposed model.

$$I(t) = \begin{Bmatrix} b_1\, W^{a_1}\left(e^{\alpha_1 V_{\mathrm{i}}(t)} - 1\right) + X\left(e^{\gamma V_{\mathrm{i}}(t)} - 1\right), & V_{\mathrm{i}}(t) \geq 0 \\ b_2 W^{a_2}\left(e^{\alpha_2 V_{\mathrm{i}}(t)} - 1\right) + X\left(e^{\gamma V_{\mathrm{i}}(t)} - 1\right), & V_{\mathrm{i}}(t) < 0 \end{Bmatrix} \quad (2)$$

$$\frac{dW}{dt} = A * V_{\mathrm{i}}{}^{m} * f(W) \qquad (3)$$

Equation (4) represents the modified window function proposed in accordance with the criterion set by Prodromakis *et.al* [3]

$$\boldsymbol{f}(W) = \begin{Bmatrix} log(1 + W)^p, & 0 \leq W \leq 0.1 \\ log(1.1)^p, & 0.1 \leq W \leq 0.9 \\ log(2 - W)^p, & 0.9 \leq W \leq 1 \end{Bmatrix} \qquad (4)$$

Results and Discussions

(I)

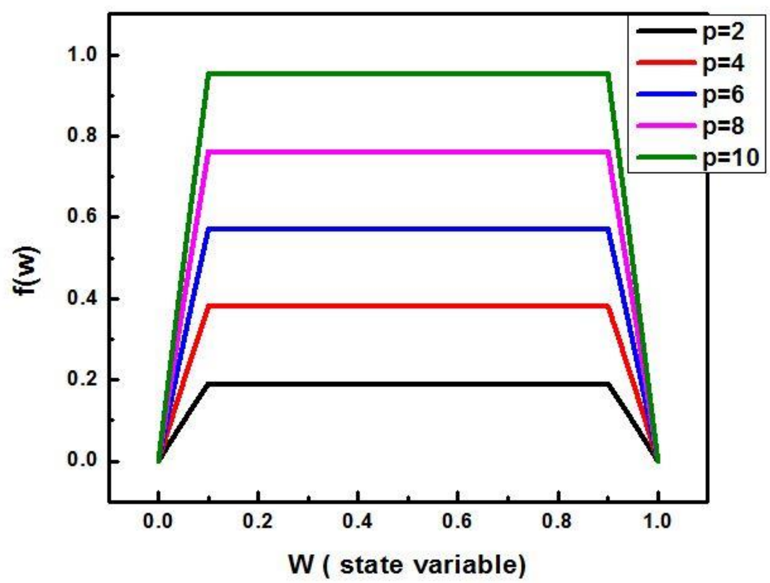

Fig.13 Window function for non- linear model

(II)

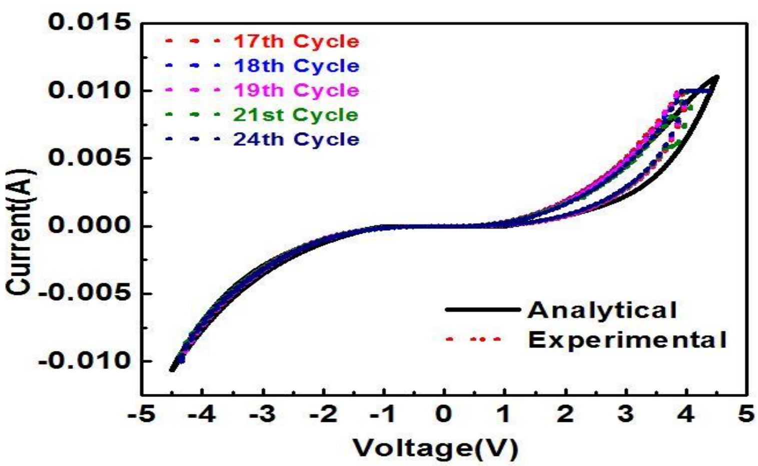

Fig.14 I-V Characteristics

Here triangular pulse of 4.5 V peak is applied at the input and I-V characteristics are obtained for different cycles. Consequently these are simultaneously plotted on ORIGIN and curve fitting is followed. Finally we arrive at the following hysteresis loops which have good correlation with the experimental data [1].

(III)

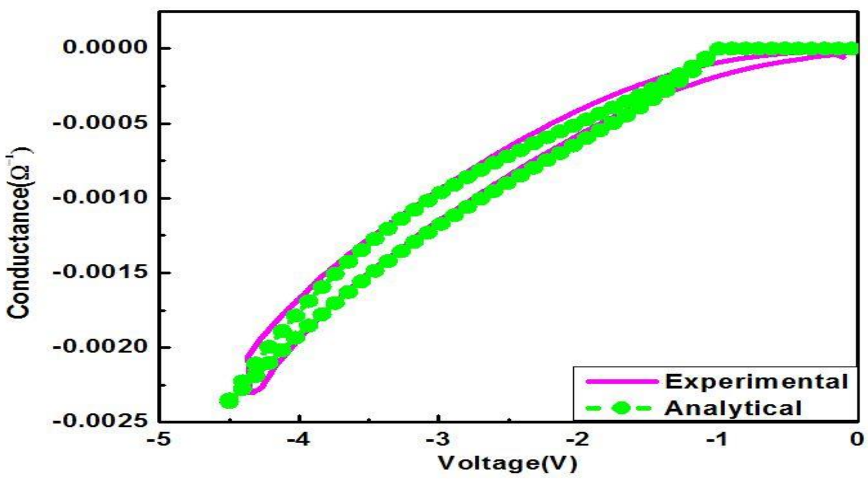

Fig.15 Conductance vs Voltage

Here conductance is calculated for both analytical and experimental response and we arrive at the given waveform after plotting on ORIGIN. The graphs are drawn in third quadrant purposefully to illustrate the significance of negative half cycles of the loops.

(IV)

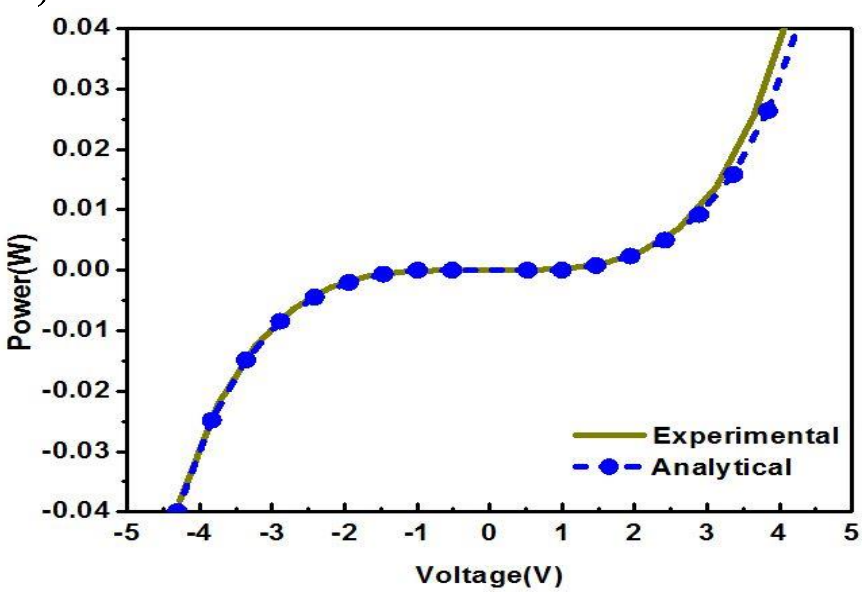

Fig.16 Actual Power vs Voltage

Due to significant switching present in the device, there is power dissipation corresponding to each level of input voltage. Thus at intervals of 0.5 V each, we calculate the average power at that level by multiplying the voltage magnitude by the average current at that level. The average power thus calculated for positive and negative cycles is thus represented in first and third quadrant respectively and matched with corresponding values of experimental data.

(V)

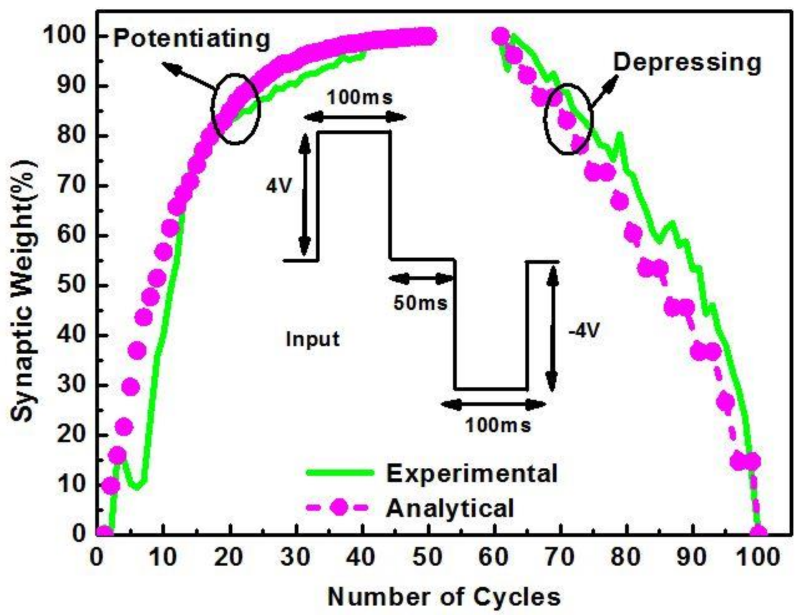

Fig.17 Synaptic behavior of the model

In order to simulate the synaptic functionality of the memristive device, we apply 50 consecutive square pulses of ON Time 100 ms followed by 50 similar negative pulses. The conductance obtained from the model is thus normalized and plotted with the experimental data. We obtain the potentiating curves (P- curve) for positive pulses and depressing curve (D) curve for negative pulses from our model as shown. As illustrated, the increasing nature of P curve is analogous to human memory learning process and the decreasing nature of D curve shows well the forgetting nature of human memory. Thus we conclude that the memristive devices show the synaptic practicality of the nature of human synapse.

(VI)

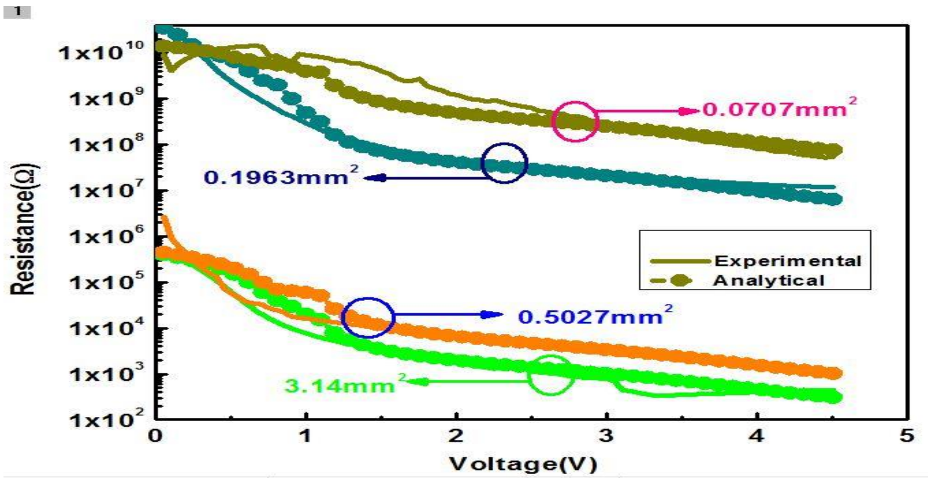

Fig.18 Resistance vs voltage for different area

As we know that area of the device plays a significant role in determining the resistance offered by the device architecture to the flow of current through the switching layer, we try to simulate the above effect by controlling the conductivity parameter in our model for various area values. The result obtained shows that the memristive devices offer high resistance at lower cross sectional areas and vice versa.

(VII)

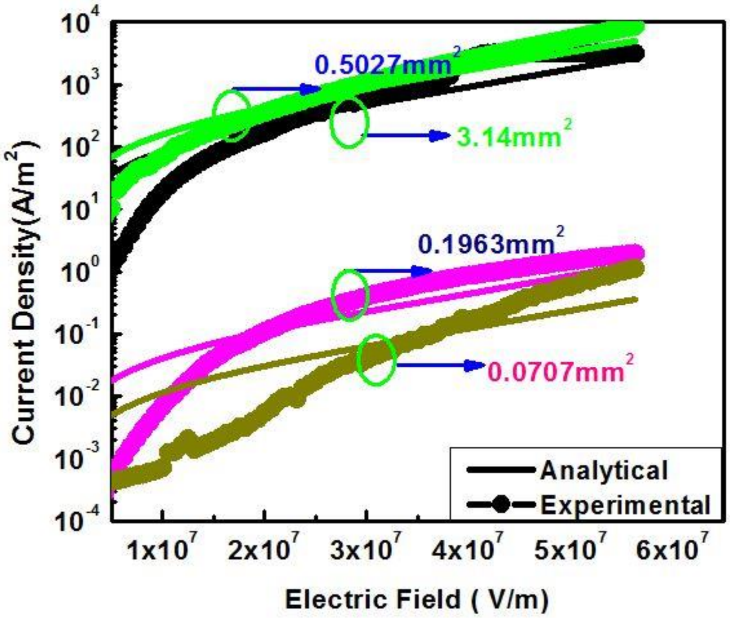

Fig.19 Current Density vs Electric field for different area

(VIII)

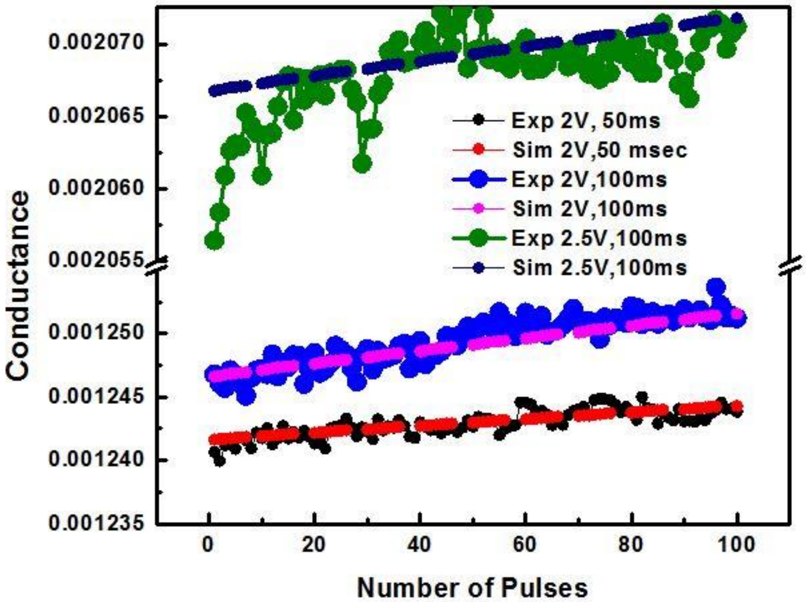

Fig.20 Conductance vs number of pulses for different inputs

Here we observe the effect of the number of pulses on the device conductance. As the magnitude of applied input pulses increases we get a higher conductance for the device. This behavior is due to higher value of current density in the device at higher input magnitude.

TABLE.2

Physical interpretation of parameters used in our model

Parameters	**Range**	**Physical Significance**
b_1,b_2	10^{-4} to 10^{-2}	Experimental fitting parameters
γ	1to 2	Diode parameters like ideality factor and thermal voltage
α_1, α_2	$\pm$0.1 to $\pm$ 0.8	Fitting parameters
a_1, a_2	1 to 5	Parameters controlling hysteresis loop broadness.
X	10^{-10}	Magnitude of ideal diode behavior
A	Arbitrary	Window function effect
m	Odd integer	Controls the effect of input voltage on the state variable

Chapter 3

Conclusion and Future Work

Here Y_2O_3 based memristive switching characteristics have been assessed based on two analytical models with a new window function and modified current voltage relationship for neuromorphic applications. Various shortcomings in the previous models such as absence of a parameter to account for asymmetric nature of the characteristics, were successfully eradicated by defining suitable parameters. Various processes of the human brain such as learning and forgetting were successfully simulated through the analytical model and the accuracy found to be considerably high (95.36 %). It is expected that the analytical models defined by us shall prove to be useful in evaluating the performance of memristive devices in various fields such as image processing and boolean logic implementation.

Chapter 4

References

1.M.Das, A.Kumar, R.Singh, M.T.Htay and S.Mukherjee "Realization of synaptic learning and memory functions in Y_2O_3 based memristive device fabricated by dual ion beam sputtering", Nanotechnology, vol. 29, no. 055203, pp. 1-9, 2018.

2. C. Yakopcic, T. M. Taha, G. Subramanyam, R. E. Pino, and S. Rogers, "A memristor device model", IEEE Electron Device Letters, vol. 32, no. 10 pp. 1436-1438, 2011.

3. T. Prodromakis, B. P. Peh, C. Papavassiliou, C.Toumazou, "A versatile memristor model with nonlinear dopant kinetics," IEEE Transaction Electron Device, vol.58, no. 9, pp. 3099-3105, 2011.

4. J. J. Yang, M. D. Pickett, X. Li, D. A. A. Ohlberg, D.R. Stewart, R. S. Williams, "Memristive switching mechanism for metal/oxide/metal nanodevices," Nature Nanotechnology, vol. 3, pp. 429-433, 2008.

5. L. Chua, "Memristor- The missing circuit element," IEEE Transaction Circuit Theory, vol. 18, no. 5, pp. 507–519,1971.